5th ECPMG Delft · 2024

Proceedings of the 5th ECPMG 2024
5th European Conference on Physical Modelling in Geotechnics
2-4 October 2024, Delft, the Netherlands

Stress redistribution around cross passages in shallow tunnels

A. SAIF, Y. CHEN, E. SORANZO, W. WU
University of Natural Resources and Life Sciences, Vienna, Austria, ahsan.saif@boku.ac.at, chenyiru@boku.ac.at, enrico.soranzo@boku.ac.at, wei.wu@boku.ac.at

ABSTRACT: Construction of cross passages is a standard practice in tunnelling, functioning as adits between the running tunnels for emergency access, maintenance, and equipment storage. The effect of cross passage excavation on the running tunnels is poorly understood and sparsely documented. This study investigates the stress redistribution around cross passages by performing centrifuge experiments on a scaled model at 50g. Uni-directional strain gauges, installed near the crown and springlines of the cross-passage opening, were used to measure the hoop and longitudinal strains and back-calculate the changes in stress in the parent tunnel. The results from centrifuge tests were then compared with three-dimensional finite element analyses considering the parent tunnel lining as linearly elastic and using Mohr-Coulomb failure criterion to model the soil.
Results indicate that linear strain gauges provide a reliable method of estimating stress changes in hoop and longitudinal directions. Current experiments show that the increase in hoop force near the opening is about 2.68 times and 1.72 times for C/D = 0.5 and C/D = 1.0 respectively. While some agreement with numerical results is observed, some values significantly differ in experiments as compared to numerical values. Bending moments show irregular results in model experiments, possibly due to the end supports intereference. The shortcomings of the current model tests are discussed and remedies are to be implemented in future works.

1 INTRODUCTION

Transport tunnels are often constructed as twin-tubes (single direction of movement in each tunnel), for safety reasons, connected through cross passages (CPs) which are usually constructed at an interval of 250 to 500 meters. These cross-passages are built for several reasons including but not limited to access between the tunnels, provide emergency exits, or used as space for any heavy equipment (ITA COSUF, 2019). Most modern transport tunnels are built using the similar principle, i.e, twin tubes (parent tunnels) connected through cross-passages (child tunnels). In practice, the safe construction of these cross-passages between twin tunnels is of paramount importance to circumvent any negative effects on the parent tunnels.

Unfortunately, the effect of construction of CPs on the parent tunnels is generally poorly understood and sparsely documented. Specifically, the magnitude in the increase in hoop and longitudinal stresses in the lining, due to CP opening, is not reported adequately. This often leads to contractors employing ground freezing or massive and overly conservative temporary structural members to support the tunnel lining near the CP and avoid any damage to the already built parent tunnel. Both methods not only increase the cost but also introduces an additional lag in the construction of the project. Some rock mass classification systems account for tunnel intersections in rocks. For instance, Bieniawski suggests using a rock mass class one step lower when designing a tunnel intersection in a particular structural area using the Rockmass Classification System. Barton et al. (1974) recommends a joint number (J_n) value of 3 times Jn and an Excavation Support Ratio (ESR) value of 1.0 for tunnel intersections. However, similar experience-based guidelines for tunnel intersections in soil are not as prevalent.

Although centrifuge tests on model tunnels have been conducted in the past (Meguid et al. 2008; idinger et al., 2011; Soranzo et al. 2015), no centrifuge tests have been conducted on tunnel cross passages thus far. As a result, literature on understanding the effect of CP construction on the parent tunnel mostly comprises numerical studies using three-dimensional finite element (FE) or finite difference (FD) analyses. Most of these studies are either case specific studies or generalized parametric studies. For example, Tsuchiyama et al. (1988) conducted elastic numerical analyses to assess the influence zone around a parent tunnel during the construction of an access tunnel. Pottler (1992) examined a representative tunnel junction configuration within the English Channel Tunnel Project to assess the need for increased support lining thickness near the intersection area. Swoboda et al. (1998) used finite element modeling to design and evaluate the stability of an intersection between the parent tunnel and an escape tunnel in the Schonberg Tunnel Project in Austria. Hsiao et al. (2005) and Sjoberg et al. (2006) employed numerical analyses to investigate the behavior of tunnel intersection areas in the Hsuehshan Tunnel in Taiwan and the Citybanan Tunnel in Stockholm, respectively. Notably, Hsiao et

al. (2005) delved into the deformational response of tunnel junctions and recommended reinforcement for specific intersection areas using a combination of numerical analyses and artificial neural networks. Forder et al. (2008) and Schikora et al. (2013) presented relevant studies showcasing the potential of optimized design using 3D numerical modeling for tunnel junctions.

More recently parametric studies were conducted to better understand the influence of a CP on its PT. Spyridis and Bergmeister (2015) parametrically investigated the effect of a perpendicular lateral breakout on the structural response of a shallow running tunnel in a 3D FE framework. The authors concluded lateral breakouts cause significant longitudinal tension in the crown-invert area, high compression in the hoop direction on the springlines in the running tunnel and the extent of stress distribution extends to about 1 diameter of the breakout opening. In a similar study conducted by Ke et al. (2019), a 3D FD sensitivity analysis was carried out to assess the impact of various factors on tunnel cross passages. The study yielded findings similar to previous research, however a particularly interesting aspect of the study was to investigate the effect of the angle at which the cross passage intersects the parent tunnel. The results revealed that at intersection angles between 75° and 90°, the cross-passage's stress distribution remained relatively stable.

Hence from previous numerical studies and engineering experience it is understood that due to CP excavation, the forces within the lining tend to arch around the opening, causing a change in the force regime at the crown and springlines of the CP. At the springlines, a concentration of compressive hoop forces occurs while at the crown a concentration of tensile longitudinal forces occurs. Since both the CP and the parent tunnels are in essence an intersection of tunnels, the problem is three dimensional in nature which requires to be modelled as either in a detailed three-dimensional FE or FD framework or as a scaled physical centrifuge model.

Therefore, this paper deals with the physical modelling of CPs in shallow tunnels constructed in soft soils to quantify the increase in hoop and longitudinal stresses within the parent tunnel. This was achieved by carrying out centrifuge tests at 50g on a model tunnel, containing a circular retractable portion placed in a soil characterized predominantly as sand. During the centrifuge flight, the retractable part of the tunnel (representing the CP) was withdrawn away from the backfilled soil using a linear actuator, replicating the excavation of a cross passage, and the expected increase hoop and longitudinal stresses in the PT were indirectly measured using strain gauges. The objective was to evaluate the magnitude of stress transfer on the parent tunnel due to CP excavation.

2 RESEARCH METHODOLOGY

Centrifuge tests were conducted on scaled models under an increased gravitational field. This increased gravity was achieved by rotating the centrifuge around its central axis, generating a centrifugal force that acted on the model and increased its weight. However, this enhanced gravitational field varies along the height of the model and depends on the distance from the centrifuge axis to the point in the model which is of interest to us. As a result, a stress gradient forms, with the area of the model above this point of interest experiencing lower stress while the area below experiences higher stress. The increase in gravitational acceleration applied to the model is a result of the rotational speed of the centrifuge, which is related to the imposed g-value and radius by the following equation.

$$RPM = \left(\sqrt{\frac{N.g}{r}}\right) \cdot \left(\frac{60}{2.\pi}\right) \quad (1)$$

Using Equation 1, the plot in Figure 1 can be obtained for g = 9.81 m/s^2, N = 50 and different values of radii, depending upon which point in the model is considered for RPM calculation. The radius value at centre of the CP was selected to be used since that is the most relevant in the current study.

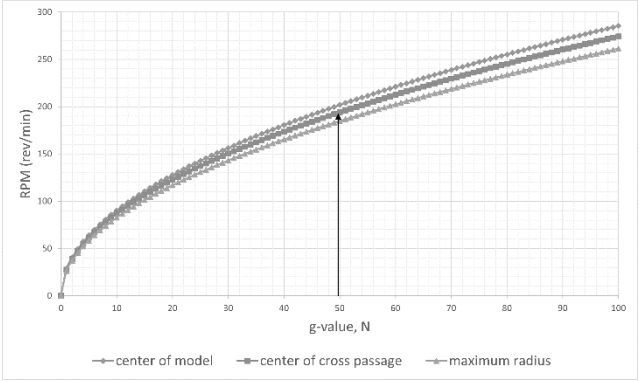

Figure 1. RPM required to reach a target g-value due to stress gradient along the model.

2.1 BOKU Centrifuge

Centrifuge tests were performed at the centrifuge testing facility of the Institute of Geotechnical Engineering (IGT) at the University of Natural Resources and Life Sciences, Vienna (BOKU). The beam-type centrifuge model manufactured by Trio-Tech (CA, USA) was installed in the late 1980s and has been successfully used in the investigation of the earth pressure distribution behind retaining structures,

foundations problems, slope stabilization measures, shallow tunnelling and other geotechnical structures (Idinger et al., 2011; Soranzo et al., 2015, Cabrera 2016, Wang et al., 2021). The centrifuge is located in a secured room dedicated for model preparation and testing. The centrifuge is encapsulated with an aerodynamic enclosure to minimize turbulence and perturbation on the rotating beam, and further provides additional protection during testing. An inside view of the centrifuge and its swinging arms is shown in Figure 2.

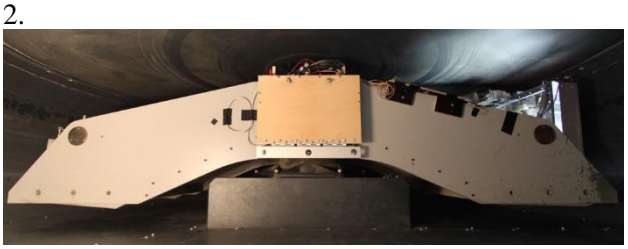

Figure 2. Inside view of the centrifuge.

2.2 Model Container

Centrifuge experiments were carried out in a specially designed testing assembly known as the model box or strong box. The model box houses the scaled model of the geotechnical structure to be analysed along with the required instrumentation and soil mass. For the present research, an aluminium model box containing a copper model tunnel (hereby referred to as the parent or model tunnel) with an extractable circular piece (here by referred to as the cross passage) was used to replicate the cross-passage excavation in a prototype tunnel. The model box was made up of three 15 mm aluminium plates and one 30 mm acrylic glass for the front wall to allow monitoring of the model during flight.The box was 440 mm in length, 155 mm in width and 400 mm high. The parent tunnel had a diameter of 100 mm in which the cross passage opening had a diameter of 50 mm, hence the parent tunnel to cross passage (CP/PT) ratio was 0.5. The parent tunnel was made from copper, representing the lining of the prototype tunnel.

The strong box contained only half of the parent tunnel, which was screwed into two aluminium stands. The cross passage was aligned with a circular cavity in the acrylic glass which allowed a linear actuator to be attached to the CP and pull it away from the parent tunnel during the experiment. A linear actuator is a step-wise motor that converts rotation into a linear motion. In this case, one rotational step was equal to 1.8°, produces a linear motion of 0.0105 mm or 10.5 µm with a thrust of 890 N. The linear actuator was controlled by a computer program through a driver, in which the input data were time interval and the number of steps. A digital cameral was used to take pictures periodically during the experiments and two LED panels, placed in front of the acrylic glass, illuminated the model box from both sides. Strain gauges were attached to the inside and outside of the parent tunnel at the springlines and crown in hoop and longitudinal directions. These were used to measure the strains at the crown and springlines of the cross passage opening during experiments, which were then converted to stress measurements. Figure 3 illustrates the model container ready to be placed in the centrifuge while Figure 4 shows the arrangement of the strain gauges (SGs) on the model tunnel. SH21 to SH23 are spaced 25 mm center to center while SH24 is placed at a distance of 50 mm from SH23.

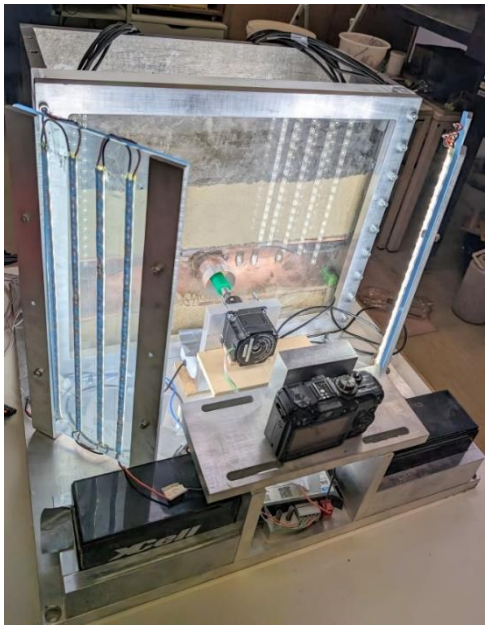

Figure 3. Model container with the required instrumentation ready to be placed in the centrifuge.

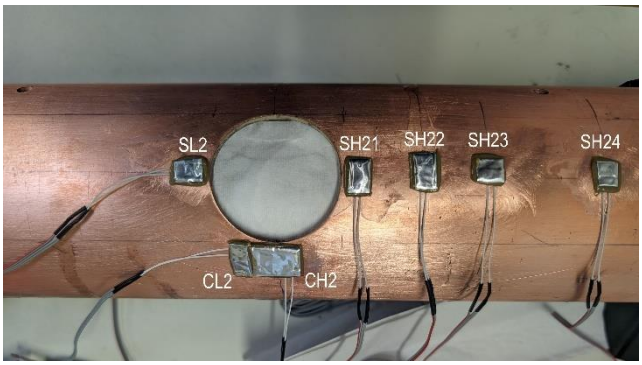

Figure 4. Arrangement of strain gauges on the model tunnel (identical on both sides).

2.3 Soil Properties

The soil used for this research endeavour was classified as a well graded sand with silt (SW-SM) according to the Unified Classification System (USCS) with a specific gravity of 2.595, determined using the picnometer method. Figures 5 and 6 illustrate

the grain size distribution and standard Proctor curve for the soil. Samples were prepared using dry soil with cover to diameter (C/D) ratios of 0.5 and 1.0. Samples were prepared by pouring dry soil and then dry tamping it in layers. The backfilled dry sand had a density of 1.60 to 1.62 g/cm^3.

Figure 5. Gradation curve of the soil.

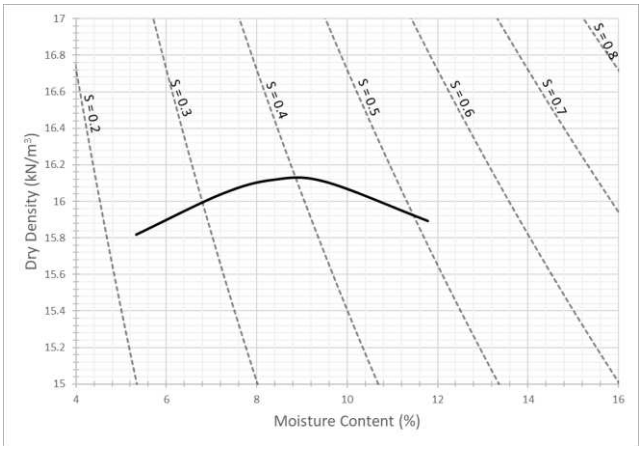

Figure 6. Standard Proctor curve of the soil.

2.4 Comparison with 3D FE Analyses

Three-dimensional finite element analyses (3D FE) in PLAXIS 3D were used as comparison to validate the results from centrifuge results. The numerical model was 100 m x 100 m x 100 m with a total of around 176407 elements and 281786 nodes as shown in Figure 7. The model was free at the top normally fixed at the lateral sides and full fixed at the bottom. Furthermore, the soil was modelled using Mohr-Coulomb (MC) failure criterion and the lining was modelled as a linearly elastic plate element. Properties for the soil and lining are listed in Tables 1 and 2. The soil was considered as a loose dry sand with a low secant modulus of elasticity. A 10 kPa cohesion was added simply to overcome convergence issues in the model. The numerical model had three phases:

1. Initial stress state developed based on gravity.
2. Soil was excavated and the parent tunnel was wished in place.
3. Cross passage opening was introduced in the parent tunnel. Further excavation of child tunnel not proceeded.
4. Results were extracted based on axial force and bending moment in hoop and longitudinal directions near the CP opening.

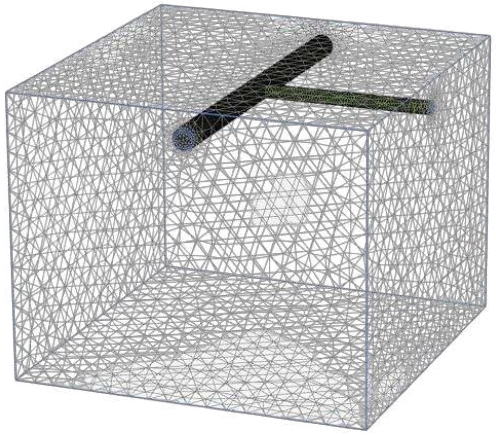

Figure 7. 3D FE Model with the parent tunnel and child tunnel.

Table 1: MC soil parameters used for 3D FE analyses.

Parameter	**Value**	**Units**
Unit Weight	16	kN/m^3
Secant's Modulus of Elasticity	10	MPa
Poisson ratio	0.3	-
Angle of Friction	30	°
Cohesion	10	kPa
Angle of Dilation	0	°

Table 2: Elastic lining parameters used for 3D FE analyses.

Parameter	**Value**	**Units**
Unit Weight	25	kN/m^3
Secant's Modulus of Elasticity	30	GPa
Poisson ratio	0.15	-
Thickness	250	mm

3 RESULTS

Results from centrifuge tests were obtained in the form of strain measurements from the strain gauges attached both on the outside and inside of the model tunnel as already shown in Figure 4. After preparing the samples, the strain gauges were zeroed before operating the centrifuge to eliminate the strains induced during sample preparation. Strains from the experiments were converted to inside-outside stresses, in the respective directions of the strain gauges (hoop or longitudinal). Accordingly, the forces and bending moments were then obtained by assuming the stress

distribution in the model tunnel as presented in Figure 8.

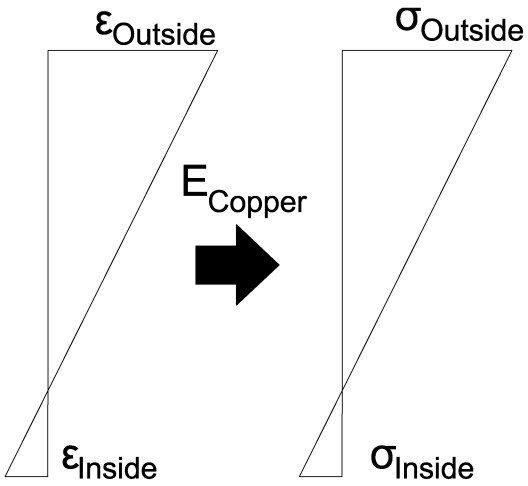

Figure 8. Assumed stress distribution in the tunnel.

3.1 Stress changes samples.

Figures 9 to 13 illustrate the results from the experiments and highlighted in red brackets is the data of the strain gauges and the time at which the CP is retracted. It can be observed that as the CP is retracted during flight, the inside SGs show a decrease in compression while the outside SGs show a decrease in tension. This change in stress is also maximum nearest to the CP opening (SH11/SH21) while least farthest from the CP opening (SH14/SH24).

Figure 11 show similar results for longitudinal strains near the springlines. The inside SG (SL1) measure a decrease in tension while the outside SG (SL2) shows a decrease in compression. The SGs in crown of the CP show very high strains, as shown in Figures 12 and 13, in both directions which could indicate damage during centrifuge flight due to soil movement pulling apart the adhesive glue applied on top of the SGs.

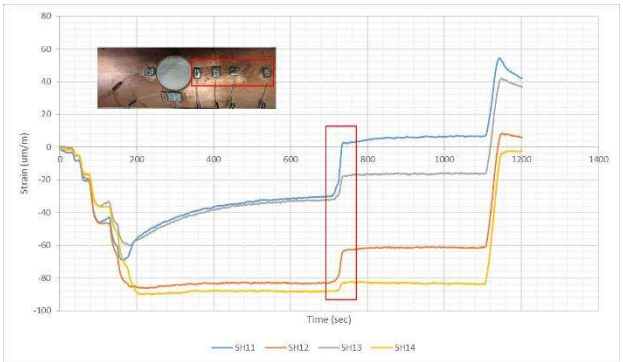

Figure 9. Outside-inside strains in hoop direction at springlines of CP (C/D = 0.5).

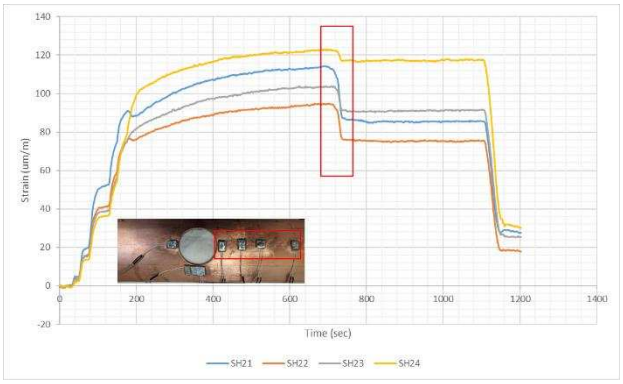

Figure 10. Outside strains in hoop direction at springlines of CP (C/D = 0.5).

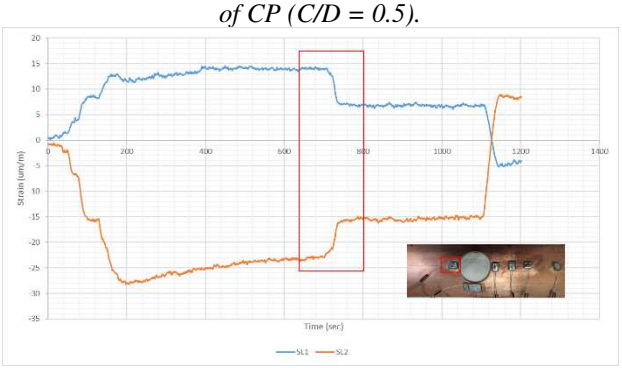

Figure 11. Outside-inside strains in longitudinal direction at springlines(C/D = 0.5).

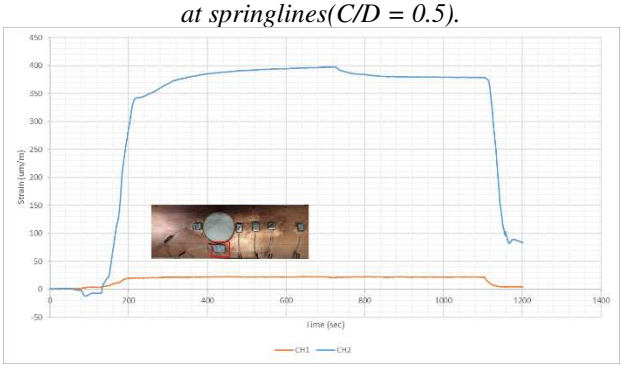

Figure 12. Outside-inside strains in hoop direction at the crown of CP (C/D = 0.5).

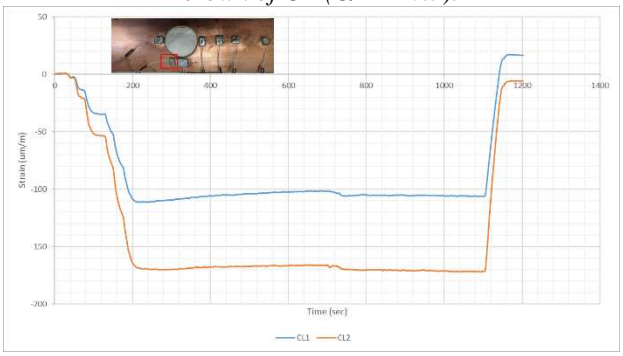

Figure 13. Outside-inside strains in longitudinal direction at the crown of CP (C/D = 0.5).

The strains were then converted into axial forces and bending moments both for hoop and longitudinal directions using equations 2 to 5. The summary of experimental results is listed in Tables 3 and 4.

Stress inside = $\sigma_i = \varepsilon_i \times E_{Copper}$ (2)

Stress outside = $\sigma_o = \varepsilon_o \times E_{Copper}$ (3)

Normal Force = N = $((\sigma_i + \sigma_o)Ac)/2$ (4)

Bending Moment = (5)

$$BM = W \cdot \left(\sigma_o - \frac{N}{A_c}\right) = W \cdot \left(\frac{N}{A_c} - \sigma_i\right)$$

where $W = bd^2/6$, b = 1 m, d = 0.25 m (thickness of lining), E_{Copper} = 125 GPa, A_C = 0.25 m^2 (area of lining)

Table 3: Centrifuge results (C/D = 0.5 after CP retraction) comparison with 3D FE.

Experimental results after CP extraction (C/D = 0.5)						**3D FE Results**	
Inside Strain	**Outside Strain**	**Stress inside**	**Stress outside**	**Force**	**Bending Moment**	**Force**	**Bending Moment**
μm	*μm*	*MPa*	*MPa*	*kN/m*	*kN.m/m*	*kN/m*	*kN.m/m*
SH11 6	SH21 85	0.75	10.62	-1421.87	-59.13	-763.8	-112.6
SH12 -61.6	SH22 75.4	-7.7	9.42	-215.62	-8.88	-215.8	-71.75
SH13 -16.75	SH23 90.3	-2.09	11.28	-1149.21	-47.76	-201	-62.58
SH14 -82.8	SH24 116.7	-10.35	14.58	-529.68	-21.91	-199.5	-60.03
SL1 6.68	SL2 -15.7	0.83	-1.96	-140.93	5.85	-138.6	-14.13

Table 4: Centrifuge results (C/D = 1.0 after CP retraction) comparison with 3D FE.

Experimental results after CP extraction (C/D = 1.0)						**3D FE Results**	
Inside Strain	**Outside Strain**	**Stress inside**	**Stress outside**	**Force**	**Bending Moment**	**Force**	**Bending Moment**
μm	*μm*	*MPa*	*MPa*	*kN/m*	*kN.m/m*	*kN/m*	*kN.m/m*
SH11 11.5	SH21 71	1.4375	8.875	-1289.06	-53.61	-1224	-180.9
SH12 -77.4	SH22 66.6	-9.67	8.32	-168.75	7.11	-346.9	-115.3
SH13 -46.8	SH23 52.1	-5.85	6.51	-82.81	-3.38	-321.5	-100.6
SH14 -149.9	SH24 197.9	-18.73	24.73	-750	-226.17	-320.3	-95.68
SL1 -62.97	SL2 53.25	-7.87	6.65	-151.87	0.83	-149.9	-16.7

During experiments, it became evident that since the CP piece was not in contact with the parent tunnel as shown in Figure 14 in its initial position (before retraction), CP piece retraction only resulted in soil failure. Meanwhile, stresses within the lining were already arching around the opening before the piece was retracted. Therefore, the strains that are recorded before CP retraction are already increased near the opening in the parent tunnel. The present experiments show that the increase in hoop force near the opening is about 2.68 times and 1.72 times for C/D = 0.5 and C/D = 1.0 respectively. The increase is calculated by comparing measurements from SH11/SH21 and SH14/SH24.

To validate this increase in stress experimentally would be to assemble an identical model parent tunnel without an opening, with all strain gauges attached in a similar arrangement. This model tunnel would provide baseline strains for comparison with strains from the model tunnel with an opening.

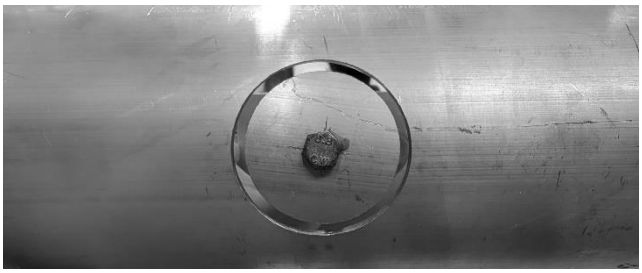

Figure 14. Space between CP piece and parent tunnel.

4 DISCUSSION AND CONCLUSIONS

This paper provides preliminary results based on centrifuge experiments which aimed to model the stress changes within the parent tunnel due to cross passage excavation and compare the results to 3D FE analyses. To this extent, centrifuge experiments were performed at 50g with dry sand using linear strain gauges as the main measuring instruments and numerical analyses were carried in PLAXIS 3D. Valuable experience regarding model building and data acquisition was obtained through this preliminary set of experiments.

From Tables 3 and 4, it can be observed that SH13/SH23 (second SG at the springlines) show very high value in C/D = 0.5 experiment and very low value in C/D = 1.0 experiment for both force and bending moment compared to SH11/SH21 and SH12/SH22, indicating it might be malfunctioning. This could be attributed to possible damage during sample preparation. Similarly, crown SGs also seem to show a huge strain due to the soil movement, causing the adhesive on top of the SGs to pull away.

Results from numerical models are also presented in Tables 3 and 4 for comparison with experimental results. It is observed that for hoop SGs in C/D = 0.5, the SH11/SH21 value from the centrifuge experiment is significantly higher than its numerical counterpart, while SH12/SH22 is nearly identical in both experiments and numerical results. SH13/SH23 and SH14/SH24 again exhibit significant differences between experimental and numerical values. Similar trends are observed for C/D = 1.0; however, SH11/SH21 and SH12/SH22 show very good agreement with numerical results. SL1/SL2 exhibit appreciable consistency between experimental and numerical results for both C/D ratios. Bending moments consistently appear lower in the experiments (with the exception of SH14/SH24 in C/D = 1.0), indicating that the ends of the model may be affecting bending moments induced in the tunnel model.

Therefore, it is suggested that SH13/SH23 and SH14/SH24, as well as the crown SGs, might need to be replaced as they could be malfunctioning. At the same time, an identical model tunnel with no CP opening will be used to acquire baseline strain values which can then be used to quantify the increase in stress for the model tunnel with a CP opening.

However, it can be concluded from these experiments that linear strain gauges provide a reliable method for estimating both hoop and longitudinal stresses within the model tunnel. Secondly, it was observed that the CP retraction piece did not maintain contact with the periphery of the parent tunnel opening, allowing stresses to arch around the opening regardless of soil failure or CP piece retraction. In terms of results quantitatively, current experiments indicate a significant increase in hoop force near the opening, with values approximately 2.68 times and 1.72 times higher for C/D = 0.5 and C/D = 1.0, respectively. While there is some alignment with numerical predictions, discrepancies between experimental and numerical values were noted, suggesting further investigation is needed to reconcile these differences. Lastly, the analysis of bending moments in model experiments revealed irregular results, potentially attributed to interference from the end supports. This aspect warrants closer examination in future experiments to better understand and mitigate such interferences.

5 FUTURE RESEARCH

A different model tunnel without an opening is envisaged to be used to acquire baseline strain values which could then be compared with strains from the model tunnel with CP opening in future experiments. Model tunnels with different sizes of CP openings will also be built in order to evaluate the effect of CP/PT ratio on the stress redistribution.

ACKNOWLEDGEMENTS

The authors thank the financial support provided by the Austrian Science Fund (FWF) under grant no. **P 34257** to help make this research project a reality.

REFERENCES

Barton, N., Lien, R. and Lunde, J. (1974) Engineering Classification of Rock Masses for the Design of Tunnel Support. Rock Mechanics, 6, 189-236. https://doi.org/10.1007/BF01239496.

Bieniawski, Z.T. (1989) Engineering Rock Mass Classifications. Wiley, New York.

Cabrera, M., A., (2016). Experimental modelling of granular flows in rotating frames. Doctoral thesis, BOKU Vienna.

Hsiao, F.,Y., Wang, C.,L., Chern, J.,C., (2009). Numerical simulation of rock deformation for support design in tunnel intersection area. Tunn Undergr Sp Technol. https://doi.org/10.1016/j. tust.2008.01.003.

Hsiao, F., Y., Yu, C., W., Chern, J., C., (2005). Modeling the behaviors of the tunnel intersection areas adjacent to the ventilation shafts in the Hsuehshan tunnel. In: Proceedings of the international symposium on design, construction and operation of long tunnels, Taipei.

Idinger, G., Aklik, P., Wu, W. et al. (2011). Centrifuge model test on the face stability of shallow tunnel. Acta Geotech. 6, 105–117. https://doi.org/10.1007/s11440-011-0139-2.

International Tunnelling Association, Committee on Operational Safety of Underground Facilities (ITA-COSUF), (2019). Current practice on cross-passage design to support safety in rail and metro tunnels. Regulations, Guidelines and Best Practice.

Meguid, M. A., Saada, O., Nunes, M. A., & Mattar, J. (2008). Physical modeling of tunnels in soft ground: A review. *Tunnelling and Underground Space Technology, 23*(2), 185-198. https://doi.org/10.1016/j.tust.2007.02.003

PLAXIS 3D Reference Manual, 2022.

Schikora, K., Piegendorfer, M., Filus, M., (2013). Plane and three-dimensional analysis in tunneling using the example of current and planned construction. Beton Stahlbetonbau 108:252–263.

Spyridis, P., Bergmeister, K., (2015). Analysis of lateral openings in tunnel linings. Tunn Undergr Sp Technol. https://doi.org/10.1016/j.tust.

Sjoberg, J, Leander, M., Saiang D (2006) Three-dimensional analysis of tunnel intersections for a train tunnel under Stockholm. In: Proceedings of the North American Tunneling 2006 Conference.

Soranzo, E., Tamagnini, R., Wu, W., (2015). Face stability of shallow tunnels in partially saturated soil: centrifuge testing and numerical analysis. Géotechnique 65, No. 6, 454–467.

Swoboda, G., Shen, X., P., Rosas, L., (1998). Damage model for jointed rock mass and its application to tunnelling. Computers and Geotechnics. https://doi.org/10.1016/S0266-352X(98)00009-3.

Tsuchiyama, S., Hayakawa, M., Shinokawa, T., Konno, H., (1988). Deformation behavior of the tunnel under the excavation of crossing tunnel. numerical methods of geomechanics. Balkema, Rotterdam, pp 1591–1596.

Pottler, R., (1992). Three-dimensional modelling of junctions at the channel tunnel project. J Numer Anal Methods Geomech Int. https://doi.org/10.1002/nag.1610160906.

Wang, S., Idinger, G. & Wu, W. (2021). Centrifuge modelling of rainfall-induced slope failure in variably saturated soil. Acta Geotech. 16, 2899–2916. https://doi.org/10.1007/s11440-021-01169-x